

Generation of Far-Infrared Radiation by Picosecond Light Pulses in LiNbO_3

Cite as: Appl. Phys. Lett. **19**, 320 (1971); <https://doi.org/10.1063/1.1653935>

Submitted: 21 June 1971 • Published Online: 22 October 2003

K. H. Yang, P. L. Richards and Y. R. Shen



View Online



Export Citation

ARTICLES YOU MAY BE INTERESTED IN

[A wideband coherent terahertz spectroscopy system using optical rectification and electro-optic sampling](#)

Applied Physics Letters **69**, 2321 (1996); <https://doi.org/10.1063/1.117511>

[Free-space electro-optic sampling of terahertz beams](#)

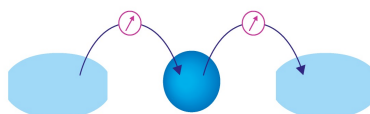
Applied Physics Letters **67**, 3523 (1995); <https://doi.org/10.1063/1.114909>

[Single-cycle terahertz pulses with amplitudes exceeding 1 MV/cm generated by optical rectification in \$\text{LiNbO}_3\$](#)

Applied Physics Letters **98**, 091106 (2011); <https://doi.org/10.1063/1.3560062>

Webinar

Interfaces: how they make
or break a nanodevice



March 29th – Register now

 Zurich
Instruments

AIP
Publishing

TABLE II. Peak characteristics (measured at 600 Hz).

Detector	λ_{peak} (μm)	Quantum efficiency	Responsivity [$10^5 \text{ V(rms)}/\text{W(rms)}$]	$D_{\lambda}^*(\lambda_{\text{peak}}, 600, 1)$ ($10^{11} \text{ cm Hz}^{1/2} \text{ W}^{-1}$) $f/1.7$	$f/6$	$f/30$
1	5.35	0.35	4.9	1.7	3.0	5.6
2	5.35	0.45	5.7	1.9	3.7	6.4
3	5.5	0.61	2.2	1.8	3.5	4.9
4	5.5	0.50	2.5	1.5	3.1	5.6

layers. This effect may have application to narrow-band detection because it reduces the effects of the background at neighboring wavelengths.

The dependence of the properties of these photovoltaic detectors on chopping frequency was investigated from 800 to 50 Hz. Due to RC limitation the responsivity and the noise increase with decreasing frequency. The detectivity remains essentially constant down to 200 Hz. At still lower frequencies the detectivity begins to decrease. This appears to be a consequence of the onset of $1/f$ noise limitation.

The present results show that epitaxial layers of PbTe can be made with adequate perfection for high-quality photovoltaic infrared detectors. Preliminary

studies indicate that these detectors may be extended to the 8–14- μm region by use of $\text{Pb}_{1-x}\text{Sn}_x\text{Te}$ layers; this work will be reported at a later date.

¹J. P. Donnelly, T. C. Harman, and A. G. Foyt, Appl. Phys. Letters 18, 259 (1971).

²K. W. Nill, A. R. Calawa, and T. C. Harman, Appl. Phys. Letters 16, 375 (1970).

³H. Holloway, E. M. Logothetis, and E. Wilkes, J. Appl. Phys. 41, 3543 (1970).

⁴H. Holloway and E. M. Logothetis, J. Appl. Phys. (to be published).

⁵The active device area may be about 10% larger than the geometrical area used here because of carrier diffusion. This would give about a 5% reduction in the values of D^* .

Generation of Far-Infrared Radiation by Picosecond Light Pulses in LiNbO_3

K. H. Yang, P. L. Richards, and Y. R. Shen

Department of Physics, University of California, and Inorganic Materials Research Division, Lawrence Radiation Laboratory, Berkeley, California 94720

(Received 21 June 1971)

We have observed far-infrared radiation generated by picosecond pulses in LiNbO_3 with several different phase-matching conditions. The output spectra, analyzed by a far-infrared Michelson interferometer and by a Fabry-Perot interferometer, agree well with theoretical calculations. The laser pulsewidth deduced from these measurements was about 2 psec in comparison with 5 psec obtained from two-photon fluorescence measurements.

The generation of coherent radiation in the far infrared (ir) by optical beating has been of considerable interest.^{1–5} Because of its broad spectral content, a picosecond laser pulse can generate far ir in a nonlinear crystal as a result of beating between its various frequency components. In this letter, we report our recent experimental results on far-ir generation in a LiNbO_3 crystal using a mode-locked Nd:glass laser.⁶ We have investigated the cases with crystal orientations corresponding to phase matching at zero frequency and at finite frequencies. In both cases, the experimental results agree well with theoretical calculations.⁷

The mode-locked laser output consisted of a train of about 30 pulses between the half-power points of the envelope with 6-nsec separation between pulses. The total energy contained in the pulse train was about 20 mJ. The pulsewidth measured with two-photon fluorescence techniques was about 5 psec. A lens with a 30-cm focal length was used to

focus the laser beam into the LiNbO_3 crystal which was 26 cm from the lens, and 1 mm of black polyethylene was used at the output to prevent laser light from reaching the far-ir detectors. The far-ir output was then split into two beams by a Mylar beam splitter. One of the beams was used for spectral analysis in either a Michelson interferometer⁸ (MI) or a Fabry-Perot interferometer⁹ (FPI) and the other for normalization. They were separately detected by two *n*-type InSb (Putley) detectors^{10,11} operated at $1.5 \pm 0.05 \text{ K}$ in a magnetic field of 5.4 kG. The entire far-ir system was evacuated to avoid water-vapor absorption. The two signals detected were amplified³ and displayed on a Tektronix 556 dual beam oscilloscope. The ratio of the two signals was then computed. To obtain the true spectrum from the Michelson interferogram, the Fourier transform of the interferogram was divided point by point by the instrumental function (the spectral sensitivity of the spectrometer-detector system).⁸

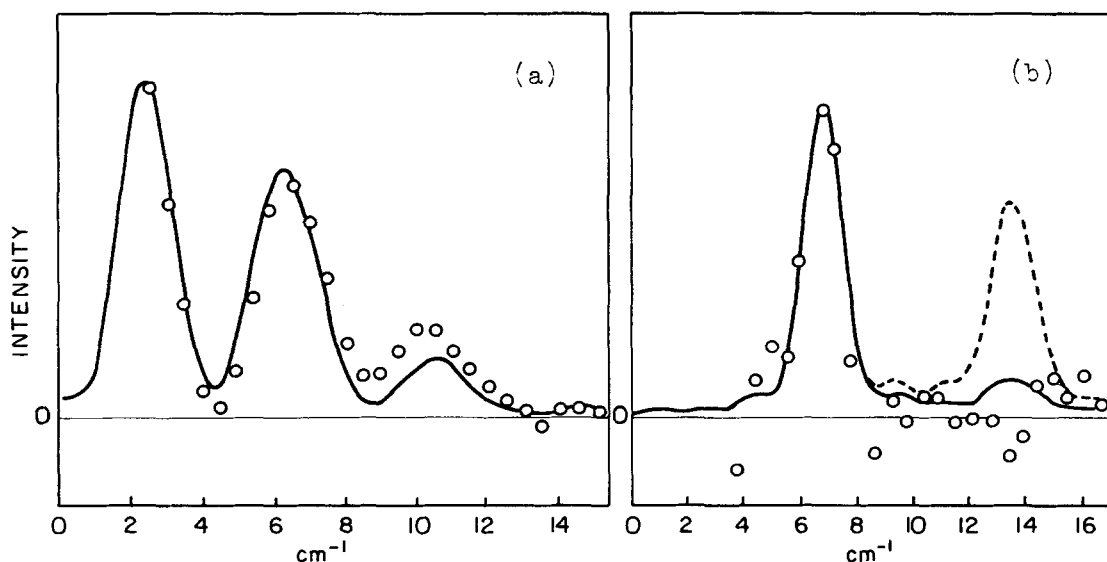


FIG. 1. (a) Far-ir spectrum generated by mode-locked pulses in LiNbO₃ phase matched at zero frequency. The experimental points were obtained from the Michelson interferogram and the solid curve from a theoretical calculation assuming Gaussian laser pulses with a 1.8-psec pulsewidth. The spectrum can be understood as a product of (1) the spectral content of the mode-locked pulses, (2) a radiation efficiency curve, and (3) a phase-matching curve centered at zero frequency (see Ref. 7). (b) Far-ir spectrum generated by mode-locked pulses in LiNbO₃ oriented to have forward and backward phase matching at 13.5 and 6.7 cm⁻¹, respectively. The experimental points were obtained from the Michelson interferogram. The solid and dashed curves were calculated by assuming Gaussian laser pulses with a pulsewidth of 2.3 and 1.8 psec, respectively. In this experiment, our laser condition was somewhat different than in the other experiments, and it was very likely that the output pulses were longer.

This instrumental function was measured by using a Hg arc lamp as a blackbody source. The same source was also used to align the MI and locate the zero of path difference.⁸

Two crystal orientations were studied. In the first, a 0.775-mm-thick LiNbO₃ crystal was oriented with the normally incident laser beam polarized along the \hat{c} axis and propagating along \hat{b} . In this configuration, the nonlinear susceptibility X_{33} ($= 1.57 \times 10^6$ esu) contributes to the generation of far ir polarized along \hat{c} , and phase matching occurs at zero difference frequency. The MI was used to investigate the far-ir spectrum. The interferogram was sampled at intervals of 0.2 mm out to a maximum of 5 mm, which limited the resolution⁸ to 2 cm⁻¹. Four laser shots were averaged for each sample. The final spectrum computed with linear apodization⁸ and corrected by the instrumental function is shown in Fig. 1(a). Because of the frequency-dependent reflection coefficient⁸ of the 5-mil Mylar beam splitter in the MI, the reliable range of the spectrum measured was from 3 to 22 cm⁻¹. The resulting spectrum contains peaks at 2.5, 6.5, and 10.5 cm⁻¹ with descending amplitude. The theoretical calculation⁷ assuming a 1.8-psec Gaussian laser pulse is also shown in Fig. 1(a) for comparison.¹² The agreement is good.

In the second case, a 1.524-mm-thick LiNbO₃ crystal was cut with its \hat{c} axis 16° away from the normal to the plane surfaces and the \hat{a} axis at 30° from the plane containing the normal and the \hat{c} axis. The nor-

mally incident laser beam was polarized to have equal components in the ordinary and the extraordinary rays. In this configuration, the ordinary far-ir output produced by $X_{24} = 1.54 \times 10^{-6}$ esu and $X_{22} = 2.2 \times 10^{-7}$ esu is phase matched at 13.5 and 6.7 cm⁻¹, corresponding to far-ir propagating in the forward and the backward directions, respectively. Extraordinary far ir was produced by X_{24} , X_{31} , X_{22} , and X_{33} , but was rejected in our experiments by a grid polarizer. The experimental result measured with the MI is shown in Fig. 1(b). The backward phase-matched peak⁷ at 6.5 cm⁻¹ was observed, but the forward phase-matched peak expected at 13.5 cm⁻¹ was not distinguishable from the background noise. Theoretical curves for 1.8- and 2.3-psec Gaussian laser pulses are shown for comparison.¹² It is seen that the relative strength of the 13.5-cm⁻¹ peak is very sensitive to the variation of the pulsewidth, which changes with the laser operating conditions. In a separate experiment, we used a far-ir FPI to analyze the spectrum. Since the spectrum is expected to contain only two narrow phase-matching peaks, an FPI which has higher peak transmissivity than the MI should be more suitable. The experimental results are shown in Fig. 2. The first, third, and fifth peaks in the figure arise from the forward phase-matched peak at 13.5 cm⁻¹, while the second and fourth peaks have contributions from both the forward and the backward phase-matched peaks. Since the resolving power of the FPI^{8,9} was limited to about 4 due to the 40° spreading angle of the far-ir radiation from the crystal, the theoret-

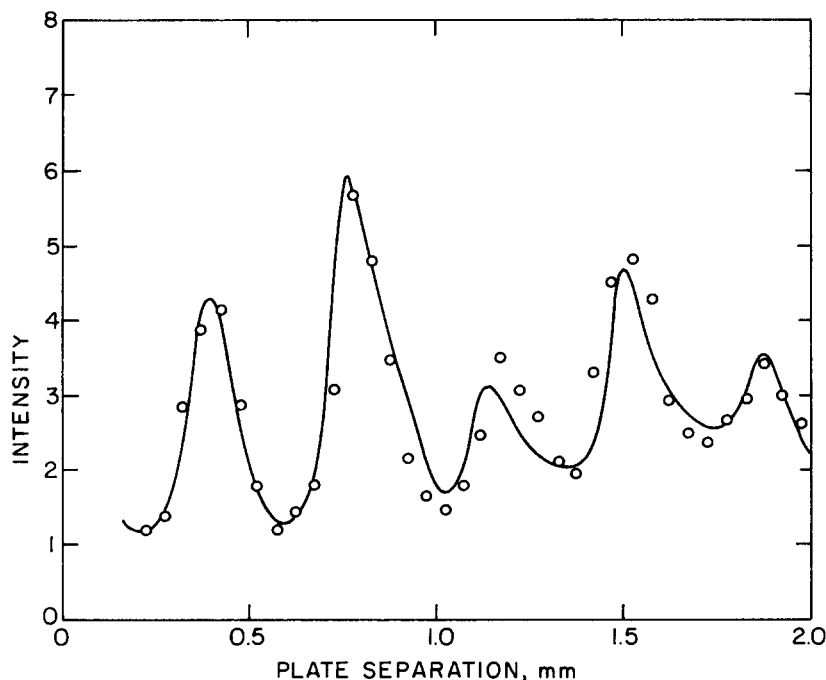


FIG. 2. Fabry-Perot fringes of far-ir radiation generated by mode-locked pulses in LiNbO_3 simultaneously phase matched at 13.5 and 6.7 cm^{-1} . The circles are experimental points and the curve was calculated from the dashed theoretical spectrum in Fig. 1(b) corresponding to Gaussian laser pulses with a 1.8 -psec pulsewidth.

cal widths ($\sim 2 \text{ cm}^{-1}$) of the phase-matched peaks were not resolved. The solid curve in Fig. 2 is the corresponding theoretical calculation of the interferometer fringes assuming Gaussian laser pulses with a 1.8 -psec pulsewidth. It appears to be in satisfactory agreement with the experimental results. As a separate check using the FPI, we rotated the LiNbO_3 crystal to phase match at $\theta = 14^\circ$. The result was similar to Fig. 2, except that the phase-matched peaks appear at 11 and 5.5 cm^{-1} as expected from the theory.

The total far-ir energy detected from X_{33} in the first case (phase matching at zero frequency) was of the order of 1 erg , which is about 20 times larger than that detected in the second case (phase matching at finite frequencies). Both agree to within an order of magnitude with a theoretical estimate based on a mode-locked laser train of 30 pulses and a peak power of 0.2 GW/cm^2 . We also measured the relative far-ir power generated by X_{31} and X_{33} . The measured ratio $X_{33}/X_{31} \approx 4$ was in satisfactory agreement with the calculated value¹³ of 3.5 . The peak power of the picosecond far-ir pulses in the first case was of the order of 200 W , which could be increased to 5 kW by increasing the laser peak power to 1 GW/cm^2 . In the second case, the spectral width and the tunability cannot compete with the two-ruby-laser system previously investigated,² but if the laser pulsewidth could be as short as 0.5 psec , this system would be capable of producing tunable far-ir pulses from 3 to 40 cm^{-1} . These pulses can be used to investigate transient and nonlinear phenomena in the far-ir region.

The authors want to thank J. Morris for calculating the theoretical curves in Fig. 1 and for many helpful discussions. Thanks are also due to J. W. Shelton

for help with the laser. We are indebted to Paul M. Bridenbaugh, Bell Telephone Laboratories, for furnishing LiNbO_3 crystals and to Dr. R. Kaplan, Naval Research Laboratory, for the InSb used to make the detectors. This work was supported by the U. S. Atomic Energy Commission.

¹F. Zernike, Jr. and Paul R. Berman, *Phys. Rev. Letters* 15, 999 (1965).

²D. W. Farries, K. A. Gehring, P. L. Richards, and Y. R. Shen, *Phys. Rev.* 180, 363 (1969); D. W. Farries, P. L. Richards, Y. R. Shen, and K. H. Yang, *ibid.* A 3, 2148 (1971).

³N. Van Tram and C. K. N. Patel, *Phys. Rev. Letters* 22, 464 (1969).

⁴F. Zernike, *Phys. Rev. Letters* 22, 93 (1969).

⁵J. M. Yarborough, S. S. Sussman, H. E. Purhoff, R. H. Pantell, and B. C. Johnson, *Appl. Phys. Letters* 15, 102 (1969).

⁶Results first presented in the Sixth International Quantum Electronics Conference, Kyoto, Japan, 1970, paper 8-6 (unpublished); See also T. Yajima and N. Takeuchi, *ibid.*, paper 8-5 (unpublished).

⁷J. Morris and Y. R. Shen, *Opt. Commun.* 3, 81 (1971).

⁸P. L. Richards, in *Spectroscopic Techniques*, edited by D. H. Martin (North-Holland, Amsterdam, 1967), Chap. 2.

⁹R. Ulrich, K. F. Renk, and L. Genzel, *IEEE Trans. Microwave Theory Tech.* MTT-11, 363 (1963).

¹⁰E. H. Putley and D. H. Martin, in *Spectroscopic Techniques*, edited by D. H. Martin (North-Holland, Amsterdam, 1967), p. 113.

¹¹The InSb has a carrier density of about $7 \times 10^{13}/\text{cm}^3$ and a mobility of $7 \times 10^5 \text{ cm}^2/\text{V sec}$.

¹²There is some discrepancy between the pulsewidths obtained from the two-photon fluorescence measurements and from the far-ir generation measurements. This is due to the different nature of the two methods. The two-photon fluorescence technique measures the autocorrelation of the actual pulse shape. If the pulse has some rapidly varying ripples on its more slowly varying envelope,

and if the photographic technique does not have sufficient resolution, then the two-photon fluorescence technique tends to yield an autocorrelation function of only the more slowly varying part. The ir generation measures the ac-

tual spectral content of the pulse and, consequently, would yield an apparently shorter pulse.

¹³A. Yariv, *Quantum Electronics* (Wiley, New York, 1967), p. 302.

APPLIED PHYSICS LETTERS

VOLUME 19, NUMBER 9

1 NOVEMBER 1971

Observation of Pulsation from a Double-Heterostructure Injection Laser Due to Lateral Optical Coupling

K. Kobayashi, H. Yonezu, F. Saito, and Y. Nannichi

Central Research Laboratories, Nippon Electric Co., Ltd., Kawasaki, Japan

(Received 28 June 1971; in final form 30 August 1971)

A new type of pulsation was observed in the output from a (GaAl)As double-heterostructure injection laser which happened to have two lasing filaments closely located to each other. We observed repetitive pulsed lasing in one filament and corresponding dipping in the other. This pulsation was interpreted to be due to lateral optical coupling between the two filaments.

In this letter, we report a new type of pulsation in the radiated output from a (GaAl)As double-heterostructure (DH) injection laser at room temperature and an interpretation is presented in terms of lateral optical coupling between two adjacent filaments. Basov¹ and Lee *et al.*² have obtained pulsed lasing output from GaAs injection lasers by nonuniform excitation along the lasing axis. They divided the cavity into two parts, one as an amplifier and the other as a saturable absorber. In contrast with this double-sectioned diode, we observed pulsation in the output from a diode which happened to have two lasing filaments located closely enough for optical coupling. We call this type of structure a coupled-cavity structure (CCS). Our observation suggests that nonuniform excitation of optically coupled multistripe-geometry lasers may cause pulsation under certain conditions.

The laser was fabricated by liquid-phase epitaxy,³ with the active region of $1 \times 90 \times 210 \mu$. It was placed in a diode mount matched to 50Ω . Pumping was made by current pulses with a pulsewidth of 18.8 or 42.5 nsec at a 100-Hz repetition rate. The near-field pattern magnified about 300 times was focused onto an avalanche photodiode. The small aperture of the detector and the large magnification permitted us to separate the radiated output from each filament.

The near-field patterns at three excitation currents are shown in Fig. 1. Two lasing filaments, whose spatial separation is about 5μ , are seen above 0.72 A. Figure 2 shows the total injection current

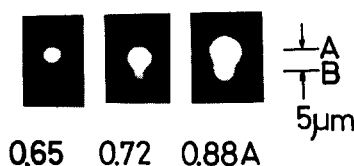


FIG. 1. Near-field patterns at three excitation currents: 0.65, 0.72, and 0.88 A from the left.

waveform (I) and the radiated output from the two filaments at the same currents as those shown in Fig. 1 (A and B). Filament A begins lasing at 0.63 A and filament B at 0.72 A. At the current level of 0.72 A, the onset of random-spike lasing of filament B and accompanying decrease in the output of stripe A were observed near the end of the pulse [Fig. 2(c)].

At higher excitation levels, pulsation occurs in the lasing output from each filament. Typical waveforms

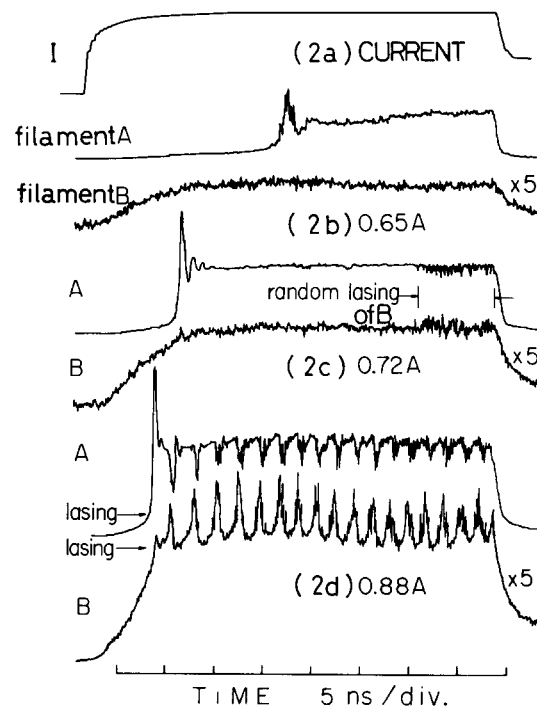


FIG. 2. Optical output of the laser. (a) Injected current waveform. (b) Current is 0.65 A; only filament A is lasing. (c) Current is 0.72 A; filament B begins lasing and corresponding dips are seen in the output of filament A. (d) Current is 0.88 A; a sustained pulsation of the output of filament B occurs with accompanying dips in the output of filament A. Time scale is 5 nsec/div.